

# COMPARISON OF FEEDBACK CONTROLLER FOR LINK STABILIZING UNITS OF THE LASER BASED SYNCHRONIZATION SYSTEM USED AT THE EUROPEAN XFEL

M. Heuer, S. Pfeiffer, H. Schlarb, DESY, Hamburg, Germany  
G. Lichtenberg, HAW, Hamburg, Germany

## Abstract

The European X-ray Free Electron Laser will allow scientists to perform experiments with an atomic scale resolution. To perform time resolved experiments at the end of the facility it is essential to provide a highly stable clock signal to all subsystems. The accuracy of this signal is extremely important since it defines limitations of precise measurement devices. A laser based synchronization system is used for the synchronization with an error in a sub-femtosecond range. These light pulses are carried by an optical fiber and exposed to external disturbances which changes the optical length of the fiber. For that reason the fiber is actively stabilized using a controller implemented on the new MicroTCA Platform. Due to the high computation resources of this platform it is possible to attack the time delay behavior of the link system with well known model based control approaches. This contribution shows how to design a model based controller for such a system and compares the control performance of the previously used PID controller with advanced control algorithms at the currently installed laboratory setup.

## INTRODUCTION

The European X-ray Free-Electron Laser (XFEL), is currently under construction at the Deutsches Elektronen Synchrotron (DESY) in Hamburg, Germany. This device with a length of 3.5 km will generate extremely intense and short X-ray laser light pulses with a duration of a few femtoseconds. Technical specifications of the facility can be found in [1]. The intense and ultra-short X-ray laser pulses are generated by an electron bunch which is feed through an undulator. They will provide scientists from all over the world the possibility to take a closer look into tiny structures on an atomic scale with a repetition rate of up to 4.5 MHz. This provides the ability to e.g. film the folding and formation of complex biomolecules [2]. One of the main challenges is to distribute a timing signal with a frequency error of less than 10 fs for all devices within the free-electron laser to achieve the required precision. In [3] a laser based synchronization system was proposed for that purpose, it is used for FLASH, and will be implemented for XFEL [4].

This paper is organized as follows: The first section gives an overview of the Laser based Synchronization system (Lb-Synch) and explains the Links Stabilization Unit (LSU). The second chapter introduces at set of possible control strategies and the dead time compensation. The experimental results and a comparison between the controller is given in section three. The paper closes with a short outlook how to improve the performance further.

## Laser Based Synchronization System

Figure 1 shows a simplified version of the laser based synchronization system with the beamline. The injector laser triggers a detachment of electrons at the cathode of the gun, which generates an electron bunch. This bunch is then accelerated by 101 superconducting modules (I0 and I39H, A1.M1-4, . . . , A25.M1-4). At the end of the beamline the bunch is lead through the undulator, which forces the electron bunches on a sinusoidal trajectory. This causes the so-called Self-Amplified Spontaneous Emission (SASE) process, which generates the high energy X-ray pulse. Other important devices within the beamline are e.g. the Bunch Arrival time Monitors (BAM) [5], which are used to measure the relative time of the electron bunch crossing a certain position w.r.t. the timing pulse of synchronization system.

To provide a clock signal to these devices the laser based synchronization system is used. It consists of two parts, the Master Laser Oscillator (MLO) generates the laser pulse train at a frequency of 216.66 MHz. This is the timing signal of the system, which is distributed through fibers to the different end station in the facility. This fiber is exposed to temperature and humidity changes as well as vibrations, which results in small changes of its optical length. To stabilize this length, the second part of this system, the so-called Link Stabilizing Unit (LSU) is used.

The lower right part of Fig. 1 shows the control scheme of a LSU. If a pulse enters the LSU, one small fraction of the laser pulse is branched off and the main part goes through a piezo stretcher into the fiber and further to the device in the accelerator. A piezo stretcher allows to slightly change the length of the fiber, hence it is used as an actuator in this scheme. At the device the pulse is partly reflected by an Faraday Rotating Mirror (FRM) and travels back the way to the LSU. This returning pulse and the fraction of the subsequent pulse pass an Optical Cross Correlator (OXC) two times. Each time a new pulse of the shape of the correlation of both incoming pulses is generated. Inside the OXC both polarizations have a different velocity and therefore both new correlation pulses are different. A balanced detector can measure the timing difference between both incoming pulses by measuring the intensity difference of the correlation pulses. If the pulses within the pulse train are equidistant and the signal of the balanced detector is zero, the length of the attached fiber is a multiple of the MLO repetition rate. With this scheme it is possible to suppress the error of the timing signal induced by length changes of the fiber caused by stress, temperature and/or humidity changes acting on the fiber.

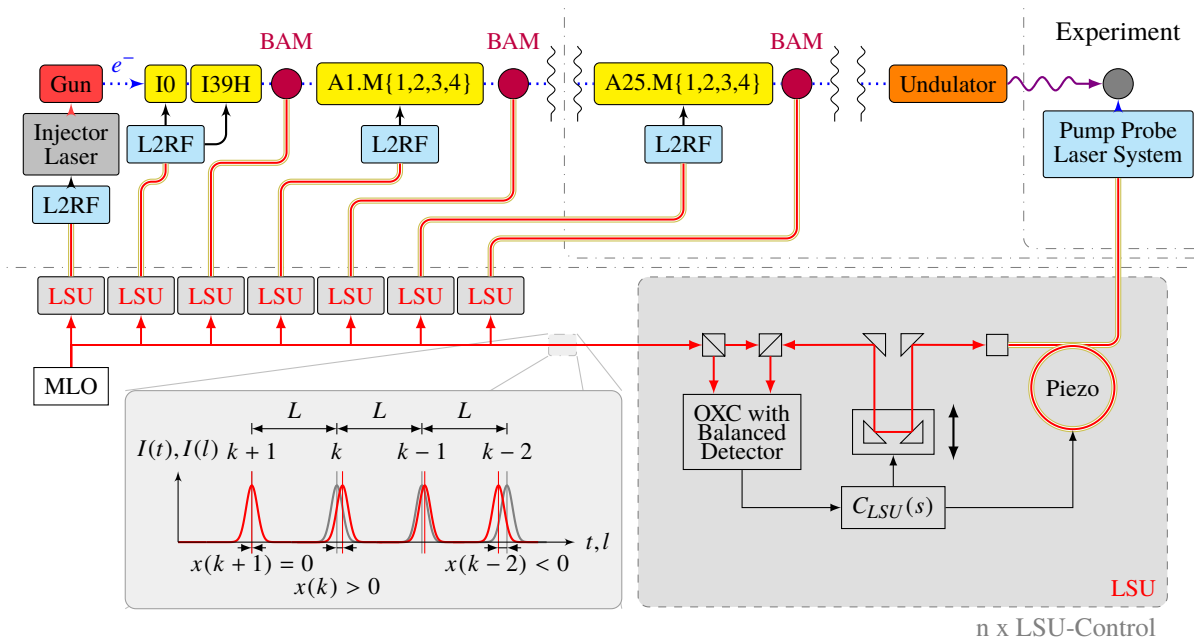


Figure 1: Block Diagram of the Laser based Synchronization System.

Link Stabilizing Unit

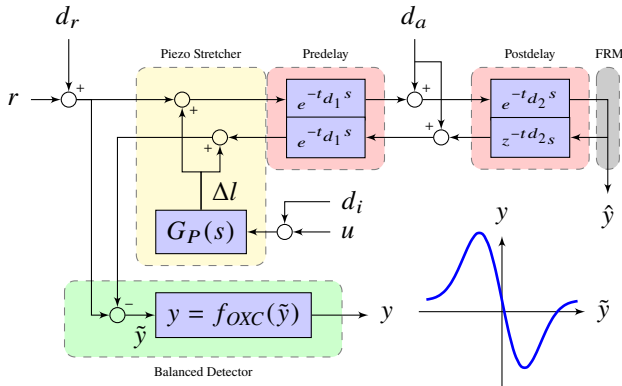


Figure 2: Block Diagram of the LSU.

The block diagram of the Link Stabilizing Unit is given in Fig. 2. All signals in this diagram are relative timing changes of the current laser pulse with respect to perfect pulse at the same time instance. A model of the piezo actuator is given by the transfer function  $G_P(s)$ , the time delay effect of the fiber link by the delay blocks and the combination of optical cross correlator and balanced detector is given by the nonlinear function  $f_{OXC}$ . In this paper we assume, that we are in the linear range of this function. The plant  $P(s)$ , where  $s$  denotes the Laplacian operator, has the input  $u$  and the output  $\hat{y}$ . For a very short link length the the transfer function of  $P(s)$  is given by  $2 \cdot G_P(s)$ , whereas if the link length increases the second response is delayed and changes the dynamic behavior.

General Control Loop

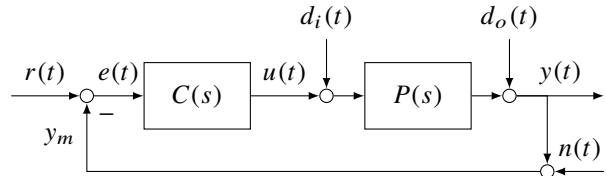


Figure 3: General setup of a control loop [6].

The general control loop is shown in Fig. 3. The two main elements are the plant  $P(s)$  with the output  $y(t)$  and the controller  $C(s)$ . The controller should generates a signal to the input of the plant  $u(t)$  in such a way, that the difference between the plant output and a given reference  $r(t)$ , called the control error  $e(t)$ , goes to zero. Moreover unwanted disturbance and noise effects which influences  $y(t)$  should be suppressed. Those effects are:

1. The input disturbance  $d_i(t)$  effects the value  $u(t)$ , e.g.
  - Ripple and other effects on the supply voltage
2. The output disturbance  $d_o(t)$  directly effects the controlled value  $y(t)$ , e.g.
  - Movement of the coarse tuning motor
  - Vibrations and temperature changes of the optical table on which the optical setup is mounted
  - Vibrations of the fiber inside the accelerator
3. The noise  $n(t)$  effects the measurement but not the controlled value  $y(t)$ , e.g.
  - Thermal noise of the photo diode
  - Noise and quantization errors of the ADC

*PID Controller*

In the current setup a proportional integral derivative (PID) controller is used to stabilize the timing error of the link. This well known controller type uses the amplified control error as well as the integration and derivation of the control error to generate the required plant input. It is easy to obtain a sufficient performance for a wide class of plants via heuristic tuning or with tuning rules from [7] even without the knowledge of the plant. For that reason this controller type is most commonly used in the industry, like shown in [8].

In this paper a PID controller will be used as a reference for the model based LQG controller.

*LQG Controller*

The linear quadratic gaussian (LQG) controller is well known in control theory and combines an optimal state observer with an optimal state feedback gain.

In the following, all systems  $P(s), C(s), \dots$  are represented in the state space form,

$$\dot{x}(t) = Ax(t) + Bu(t), \tag{1}$$

$$y(t) = Cx(t) + Du(t), \tag{2}$$

and abbreviated with

$$P(s) = \left[ \begin{array}{c|c} A & B \\ \hline C & D \end{array} \right], \tag{3}$$

where  $x(t) \in \mathbb{R}^n$  are the states (internal energy storage's),  $u(t) \in \mathbb{R}^m$  the inputs and  $y(t) \in \mathbb{R}^l$  the outputs of a system. The matrices  $A \in \mathbb{R}^{n \times n}$ ,  $B \in \mathbb{R}^{n \times m}$ ,  $C \in \mathbb{R}^{l \times n}$ ,  $D \in \mathbb{R}^{l \times m}$  representing the dynamic behavior of the system. The linear quadratic regulator (LQR) is an optimal controller of the form  $u(t) = -Fx(t)$  which minimizes the cost function

$$V = \int_0^\infty x(t)^T Qx(t) + u(t)^T Ru(t) dt, \tag{4}$$

$$Q \in \mathbb{R}^{m \times m} \geq 0, \quad R \in \mathbb{R}^{n \times n} > 0, \tag{5}$$

where  $x(t)$  are the states and  $u(t)$  are the inputs of the closed loop system. The matrices  $Q$  and  $R$  are tuning parameter and can be freely choose if they satisfy (5).

The optimal feedback gain  $F$  is computed with Matlab by

$$F = \text{lqr}(A, B, Q, R);$$

With this controller it is possible to change the eigenvalues of the closed loop system, i.e. the dynamic behavior of the system. [6]

In most cases not all states  $x(t)$  are measurable. Therefore one has to estimate them using an observer

$$O(s) = \left[ \begin{array}{c|c} A - LC & B \quad L \\ \hline I & 0 \quad 0 \end{array} \right], \quad u_o(t) = \begin{bmatrix} u(t) \\ y(t) \end{bmatrix}, \tag{6}$$

which computes the states from the known input  $u(t)$ , the measurement  $y(t)$  and the known system defined by the matrices  $A, B, C, D$ . The feedback gain  $L$  for the observer can be calculated by

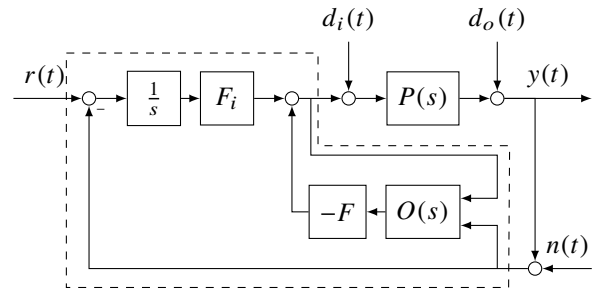


Figure 4: Block Diagram of the LSU in the current experimental setup.

$$L = \text{lqr}(A', C', Q_o, R_o)';$$

It is important to choose the observer tuning parameter  $Q_o$  and  $R_o$  in such a way, that the dynamics of the observer are faster than those of the closed loop state feedback system.

In order to reach a steady state control error of zero ( $\lim_{t \rightarrow \infty} e(t) \rightarrow 0$ ) it is necessary to include integral action to the controller if the plant itself is without integral behavior. Figure 4 shows the block-diagram for such a controller with the integrator ( $1/s$ ) and the additional feedback gain  $F_i$ . To design such a controller the augmented system

$$P_a(s) = \begin{bmatrix} \dot{x} \\ \dot{x}_i \\ y \\ x_i \end{bmatrix} \begin{bmatrix} A & 0 & B \\ C & 0 & 0 \\ C & 0 & D \\ 0 & I & 0 \end{bmatrix} \begin{bmatrix} x \\ x_i \\ u \end{bmatrix} \tag{7}$$

can be used to design the gains  $F$  and  $F_i$  in the same synthesis step.

*Smith Predictor*

The presence of a time delay inside the plant  $P(s)$  reduces the performance of the closed loop, it is even possible that the closed loop is unstable. To compensate this delay, the well known structure in Fig. 5 is used. If the plant model  $\hat{P}$  and the time delay  $e^{-\hat{t}_d s}$  model are perfect, the time delayed system is compensated and the controller reacts on the perfectly matched plant model. Further effects, if plant and the model are not equal are analyzed in [9]. In the case of long fiber links, a smith predictor can be added if the length of the link reaches a length where the time delay of the returning pulse influences the dynamic behavior of the plant.

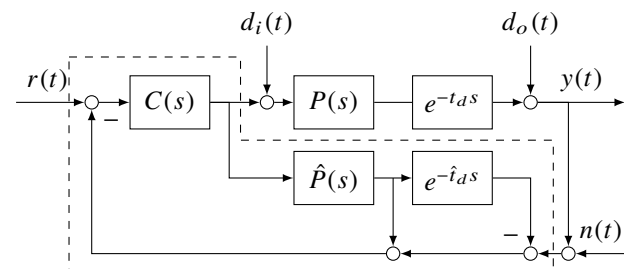


Figure 5: Control loop with a smith predictor [10].

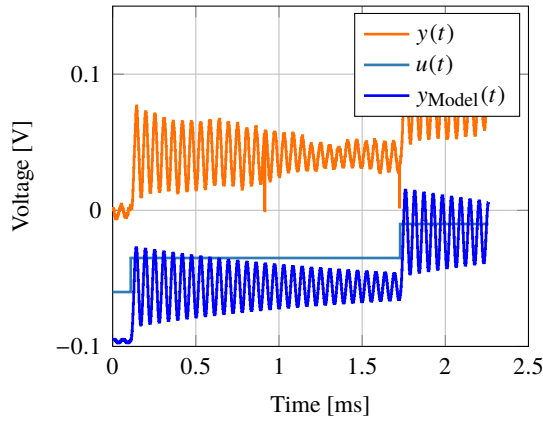


Figure 6: Validation of the identified model.

### EXPERIMENTAL RESULTS

In the following section the experimental results are presented. The control system is based on the new MicroTCA standard used for XFEL. A SIS8300L board at 81 MHz is used to compute the control algorithm and to feed the control value  $u(t)$  to the piezo amplifier. A SIS9000 connects the the balanced detector to the SIS8300L. The control algorithm itself is designed in Matlab/Simulink and is implemented on an FPGA using the Simulink to VHDL Toolchain developed in [11]. This tool is based on the SysGen Toolbox by Xilinx which is extended to a fully automated code generation and deployment environment for FPGA based MicroTCA board.

The first step of a model based controller design is to identify and verify a suitable model for the plant. In this case a black box identification is performed. An excitation signal is applied to the plant input  $u(t)$  and the response of the plant  $y(t)$  is measured. With those measurement it is possible to derive the continuous time state space model

$$A = \begin{bmatrix} -253.8 & 1.133 \cdot 10^5 & 935.9 \\ -1.133 \cdot 10^5 & -1138 & -2017 \\ 935.9 & -4035 & -1.346 \cdot 10^5 \end{bmatrix},$$

$$B = \begin{bmatrix} 112.9 & 237.9 & -209.5 \end{bmatrix},$$

$$C = \begin{bmatrix} 225.8 & -475.9 & -418.9 \end{bmatrix}$$

with  $A$  as the system matrix,  $B$  as input matrix and  $C$  as output matrix, for the 300 m link currently setup in the laboratory. The direct feedthrough matrix  $D$  is set to zero, the usual case for physically realizable plants. Figure 6 shows the validation of this model. The dynamic behavior as well as the decay of the model matches well with the measurement  $y(t)$ . The remaining offset is caused by a very slow drift behavior of the link and will be treated with an integral behavior of the controller.

In the next step we compare the dynamic behavior of both controllers.

For a minimum rms value at the output  $y(t)$  just the integrator of the PID controller is used. This value is increased as long as no oscillation occur, like it is done in the past.

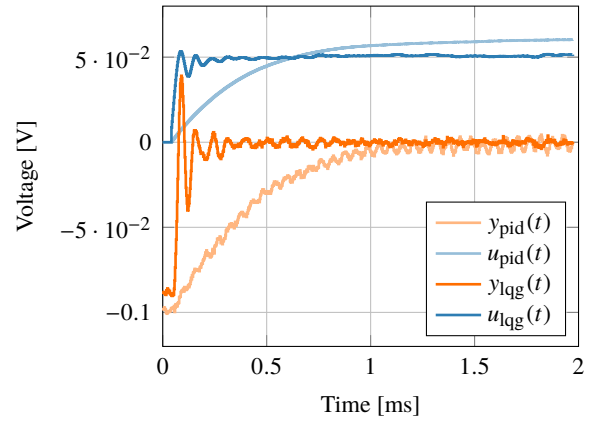


Figure 7: Dynamic behavior of the controller start.

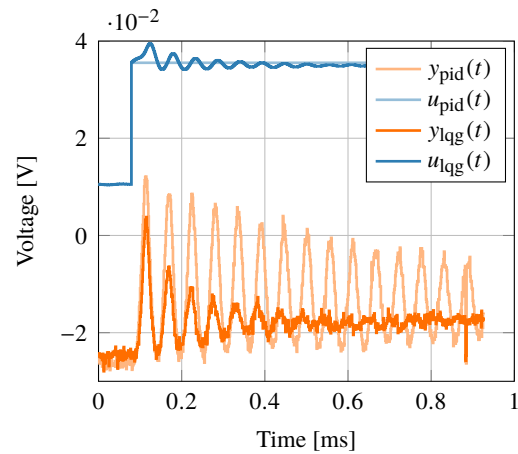


Figure 8: Response to an input disturbance  $d_i(t)$  step of the state feedback controller without integrator.

The model based LQG controller designed with the methods shown in the previous section and implemented in the FPGA.

Figure 7 shows the dynamic behavior of both controllers in the moment of the start. One can see that the LQG controller acts faster and reaches the steady state much earlier than the PID controller. In this measurement the LQG controller starts much closer to the final value. Nevertheless, the PID controller also requires more time to reach the final value if different initial values are considered. The reason for that is, that the LQG controller provides a component which directly acts on the change of the value and doesn't need time to act like an integrator would do.

The effect of the state feedback is shown in Fig. 8. Due to the knowledge of the plant, it is possible to change the eigenvalues of the closed loop system in such a way, that the dynamics have the required properties. In the case of the fiber links we would like to suppress the oscillation of the piezo crystal. Figure 8 shows exactly this behavior. With the activated controller the damping of the system is much faster.

The dynamic behavior of the LQG controller with an integrator is shown in Fig. 9. The state feedback part of the

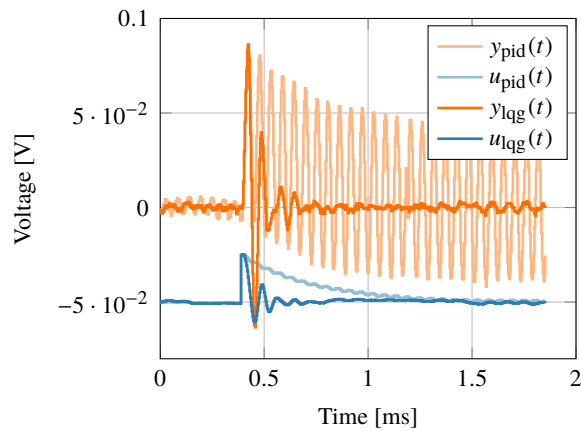


Figure 9: Response to an input disturbance  $d_i(t)$  step of the augmented state feedback controller with integrator.

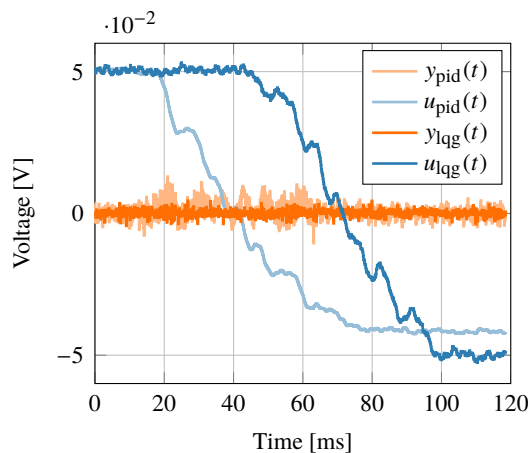


Figure 10: Response to a step of the coarse tuning motor, down-sampled by 42,  $u_{lqg}(t)$  and  $u_{pid}(t)$  are shifted to keep the graphs within the figure.

controller suppress the oscillation whereby the integration part pushes the output value  $y(t)$  back to the reference value  $r(t) = 0$ . The PID controller also reaches a non offset steady state but oscillations of the piezo crystal are not attacked in an appropriate way.

The piezo crystal, used in the LSU control scheme, adjusts the length of the fiber. This helps to cope with the disturbances mentioned earlier. The range of this actuator is limited and a motorized delay stage is used to adjust larger timing variations by a stepper motor. This behavior is shown in Fig. 10. The PID controller is too slow to suppress the

influences due to the motor, whereas the fast response of the LQG controller is suitable to cope with this influences and no changes on the output  $y(t)$  are visible.

## CONCLUSION

In this paper a model based LQG controller design with integral action is shown. Furthermore, a smith predictor is included to cope with time delayed signals. The controller is tested at the Stabilizing Fiber Links in the experimental laboratory setup. The time domain responses to disturbances shows that such a model based LQG controller is well suitable for such a system and has a superior performance with respect to a heuristically tuned PID controller.

## REFERENCES

- [1] M. Altarelli et al., XFEL, The European X-Ray Free-Electron Laser, Technical design report, DESY, Hamburg, Germany, 2007.
- [2] C. M. Günther et al., Sequential femtosecond X-ray imaging, Nature Photonics 5, 2011, pp. 99-102.
- [3] J. W. Kim et al., Large scale timing distribution and RF-synchronization for FEL facilities, FEL Conference 2004, Trieste, Italy, 2004.
- [4] Sebastian Schulz et al., Past, Present and Future aspects of Laser-Based Synchronization at FLASH, Proceedings of the International Beam Instrumentation Conference 2013, Oxford, U.K., 2013.
- [5] M. K. Bock, Measuring the Electron Bunch Timing with Femtosecond Resolution at FLASH, University of Hamburg, Hamburg, Germany, 2012.
- [6] S. Skogestad, I. Postlethwaite, Multivariable Feedback Control: Analysis and Design, Wiley, Chichester, U.K., 2001.
- [7] J. B. Ziegler, N. B. Nichols, Optimum settings for automatic controllers, ASME Transactions, v64 (1942), pp. 759-768.
- [8] H. Takatsu, T. Itoh, M. Araki, Future needs for the control theory in industries — report and topics of the control technology survey in Japanese industry.
- [9] J. E. Normey-Rico, E. F. Camacho, Control of Dead-time Processes, Springer, London U.K., 2007.
- [10] O. Smith, Closer control of loops with dead time, Chem. Eng. Progress, vol. 53, no. 5, 1957, pp. 217-219.
- [11] P. Predki, M. Heuer, L. Butkowski, A. Napieralski, Rapid FPGA development framework using a custom Simulink library for MTCA.4 modules, 19th IEEE Real Time Conference, Nara, Japan, 2014.